Published in final edited form as:
Head Neck. 2014 November ; 36(11): 1619–1627. doi:10.1002/hed.23502.

PRECLINICAL SAFETY AND ACTIVITY OF RECOMBINANT VSV-IFN-B IN AN IMMUNOCOMPETENT MODEL OF SQUAMOUS CELL CARCINOMA OF THE HEAD AND NECK

Vittal VS Kurisetty, PhD[1,A,*], **Joshua Heiber, PhD**[4,B,*], **Rae Myers**[3], **Guilherme S. Pereira, MD**[1,C], **Jarrard W. Goodwin, MD**[2], **Mark J. Federspiel, PhD**[3], **Stephen J. Russell, MD, PhD**[3], **Kah Whye Peng, PhD**[3], **Glen Barber, PhD**[1,4,*], and **Jaime R. Merchan, MD**[1,2,*]

[1]Division of Hematology & Oncology, University of Miami/Miller School of Medicine, Miami, FL

[2]Division of Otolaryngology, University of Miami/Miller School of Medicine, Miami, FL

[3]Department of Molecular Medicine, Toxicology and Pharmacology Laboratory, Mayo Clinic, Rochester, MN

[4]Division of Cell Biology, University of Miami/Miller School of Medicine, Miami, FL

Abstract

Background—VSV-IFN-β, a recombinant vesicular stomatitis virus expressing interferon-β, has demonstrated antitumor activity in vitro and in vivo. In preparation for clinical testing in human squamous cell carcinoma (SCC) of the head and neck, we conducted preclinical studies of VSV-IFN-β in syngeneic SCC models.

Methods and Results—In vitro, VSV-IFN-β (expressing rat or mouse IFN-β) induced cytotoxicity and propagated in rat (FAT-7) or mouse (SCC-VII) SCC cells during normoxia and hypoxia. In vivo, intratumoral administration of VSV-rat-IFN-β or VSV-human-IFN-β in FAT-7 bearing or non-tumor bearing immunocompetent rats did not result in acute organ toxicity or death. VSV-r-IFN-β replicated predominantly in tumors and a dose dependent anti-VSV antibody response was observed. Intratumoral or intravenous administration of VSV-IFN-β resulted in growth delay and improved survival compared to controls.

Conclusions—The above data confirm safety and feasibility of VSV-IFN-β administration in immunocompetent animals and support its clinical evaluation in advanced human head and neck cancer.

Keywords

Squamous cell carcinoma; Vesicular Stomatitis Virus; biodistribution; preclinical studies; syngeneic models

Correspondence should be addressed to: Jaime R. Merchan. 1475 NW 12 Ave. Miami, FL 33136. jmerchan2@med.miami.edu.
*Equal Contribution
[A]Current Address: Texas Tech University Health Science Center. 5001 El Paso Drive. El Paso, TX 79905.
[B]St Jude Children's Research Hospital. 262 N. Danny Thomas Place. DTRT 4046 MS# 342, Memphis TN 38105.
[C]Instituto do Cancer do Estado de Sao Paulo-University of Sao Paulo. Avenida Doutor Arnaldo, 541. Sao Paulo, Brazil 01246-000.

This work was presented at the 2011 American Association for Cancer Research Annual Meeting.

INTRODUCTION

It is estimated that 52,610 new cases of head and neck cancer (HNC), and 11,400 deaths will occur in 2012, in the USA [1]. Recent advances in the multimodality treatment of this disease have significantly improved organ preservation and quality of life [2, 3]. Modest improvement in 5-year survival for all sites has been due largely to improved outcomes in patients with cancer of the oropharynx, consistent with the evolving changes in etiology for that site [4]. In spite of these advances, between 15 and 50% of patients treated with multimodality treatment recur within 2 years [5–9], most commonly at the primary site or in the neck, and outcomes for these patients are poor with currently available treatment options. Therefore, there is an urgent need to develop novel, effective therapies for patients with refractory HNC. Because the pattern of recurrence for HNC is predominantly locoregional, this disease serves as a model for tumor directed strategies aiming at improving local control, either alone, or in combination with systemic therapies.

Oncolytic virotherapy is a strategy that exploits the natural ability of viral vectors to preferentially infect, replicate, and induce potent cytotoxicity in cancer over non-cancer cells [10]. Many oncolytic viral vectors can be genetically modified to carry genes that improve safety or antitumor effects. Examples include adenovirus, herpes simplex virus, reovirus, measles virus and vesicular stomatitis virus, among others [10, 11]. Several of the above viral vectors are being evaluated in clinical trials in patients with advanced HNC.

Vesicular stomatitis virus (VSV) is an RNA virus that belongs to the family of rhabdoviridae [12]. It induces potent in vitro and in vivo tumor cytotoxic effects, and its efficacy has been tested in a number of xenograft and syngeneic models. Preclinical studies have demonstrated activity of recombinant VSV alone or in combination with chemotherapy in murine and human models of squamous cell carcinoma (SCC) of the head and neck [13–15]. VSV-induced neurotoxicity, however is dose limiting [16, 17], limiting clinical development efforts of this agent. To attenuate VSV toxicity, we have developed a recombinant VSV that carries the gene encoding interferon beta (VSV-IFN-β), which has shown improved safety profile while keeping its in vitro and in vivo oncolytic effects [18]. In addition, IFN-β expression in the tumors may improve the antitumor efficacy due to intrinsic antiproliferative effects of interferon [19, 20].

VSV-h-IFN-β (expressing human interferon-β) is currently being developed as an oncolytic agent against hepatocellular carcinoma (Clinicaltrials.gov NCT01628640). In this report, we present the results of preclinical studies characterizing the safety, biodistribution, antiviral antibody response and antitumor efficacy of VSV-IFN-β in a syngeneic, immunocompetent rat model of SCC, in preparation for clinical evaluation of this viral vector in human squamous cell carcinoma of the head and neck..

MATERIALS AND METHODS

Cell Culture

Mouse (SCC-VII) and rat (FAT-7) SCC cell lines were obtained from ATCC (Manassas, VA) and maintained in DMEM medium with 10% fetal bovine serum (FBS) and 1%

penicillin & streptomycin (1% P/S), and Ham's F12K medium with 0.01 mg/ml insulin, 250 ng/ml hydrocortisone and 0.0025 mg/ml transferrin, 10% FBS, respectively. BHK-21 cells were maintained in Dulbecco's modified essential medium supplemented with 10% FBS (MediaTech, Inc, Manassas, VA), 100 U of penicillin G/ml, 100 U of streptomycin/ml, and 0.25 μg of amphotericin B. All cells were kept at 37°C in a humidified 5% CO_2 incubator.

Virus generation and expansion

Recombinant VSVs expressing human (VSV-h-IFN-β), mouse (VSV-m-IFN-β) and rat (VSV-r-IFN-β), were generated and propagated as previously described [18, 21]. Viruses were frozen at − 65° C or lower until use. Viruses were diluted in sterile normal saline to the desired concentration and kept on ice until use for in vitro and in vivo experiments. Virus titer was verified by 50% tissue culture infective dose ($TCID_{50}$) titration on VERO or BHK-21 cells (for in vivo safety and biodistribution experiments) or by plaque dilution (for in vitro and in vivo efficacy experiments), as previously described [22, 23].

Assessment of in vitro cytopathic effects

Cells were plated in 6-well plates (1×10^6/well)and then infected with VSV-r/m/h-IFN-β at different multiplicity of infection (MOI), depending on the experiment, for 1 h at 37°C in 2 mL of Opti-MEM® reduced serum media (Invitrogen, Carlsbad, CA). Fresh media was then added, for the respective cells and they were incubated for 24, 48 or 72 h post infection. At each time point, cell viability and cytotoxicity were measured at using the Trypan blue exclusion analysis [24–27]. Cytotoxicity experiments were performed in normoxic and hypoxic conditions. Hypoxic conditions (0.3% O2) were generated with the use of a hypoxia chamber (Coy Lab Products, Grass Lake, MI).

Western blotting

FAT-7 cells and SCC-VII cells (1×10^6) were seeded in a six well plate and infected and incubated with viruses at 1 hr and at an MOI of 5 and 10 PFU per cell and incubated for 24 hrs in serum free Opti-MEM® (Invitrogen, Carlsbad, CA). Cell supernatants were obtained, and protein concentration was determined using a Bio-Rad protein assay (Bio-Rad Hercules, CA). A total of 20 μg of supernatant protein was then separated by 10% SDS-PAGE (Polyacrylamide electrophoresis) and transferred to a 0.2 μM PVDF membrane (Bio-Rad Hercules, CA). Polyclonal rabbit antibodies against rat or mouse-IFN-β (Research Diagnostics Inc., Flanders, N.J.) were used as the primary antibodies. Horseradish peroxidase-conjugated anti-rabbit or anti-mouse was used as a secondary antibody (Promega, U.S.A) and detected by enhanced chemiluminescence (Pierce, Rockford, Ill.)

In vivo studies

All procedures involving animals were approved by the University of Miami and Mayo Clinic Animal Care Committee and were carried out in compliance with the Care and Use of Experimental Animals Guide issued by the American Council on Animal Care. A syngeneic model of *in vivo* rat squamous cell carcinoma in the neck area was established in immunocompetent Fischer-344 rats (female, 6–7 weeks old; Charles River Laboratories, U.S.A). FAT-7 cells, (3×10^6/ml in 100 μL of PBS) were injected subcutaneously (s.c) below

the right jaw line in the neck of Fischer-344 rats. Tumors were measured twice a week with a caliper, and when tumors reached ≥ 0.5 cm in diameter, in vivo treatment was initiated.

In vivo safety and biodistribution studies

Studies were performed in tumor and non-tumor bearing rats, to assess the toxicity of VSV-r-IFN-β or VSV-h-IFN-β at different dose levels, after intratumoral or subcutaneous administration of the test agent. Studies in non-tumor bearing rats assessed the safety of escalating doses of VSV-h-IFN-β (n=9), and the safety of VSV-h-IFN-β or VSV-r-IFN-β at a fixed dose, compared to saline administration (n=8). In tumor free rats, the test agent was administered (in a total volume of 50 μL) subcutaneously below the right jaw line. Studies in tumor bearing rats assessed the safety, biodistribution, and antibody formation of escalating doses of VSV-r-IFN-β (n=38) or VSV-h-IFN-β (n=24). Rats were randomized into different treatment groups (equal number of males and females) when tumors reached a diameter of approximately 5 mm. The test agent was administered intratumorally, in a total volume of 50 μL.

All rats were observed for toxicity throughout the duration of the study. To assess treatment related toxicity and biodistribution groups of rats were sacrificed at day 2 and at day 28/29, and tumor and organs were harvested, for analysis of toxicity and viral replication. Blood was extracted from rats at day 2 (jugular vein) and at days 28/29 (cardiac puncture) for determination of blood counts, chemistry, viremia, and antibody production, as described below.

Anti-VSV Ab ELISA

Serum samples were taken from the rats on days 2 and 28/29 after virus administration. Carbonate bicarbonate buffer (Sigma) was used as coating buffer. VSV-r/h-IFN-β (titer 2.4×10^{11} $TCID_{50}$/mL) was diluted 1:10,000. MaxiSorp (Nunc) plates were coated at 100 μL per well and placed at 2–8°C overnight. The plates were washed with 0.1% Tween 20 (Bio-Rad #170-3561) in PBS (Bio-Rad), 200 μL per well, 3 times. 10X Casein (Vector Labs) was diluted to 1X and added to plates to block at 100 μL per well for 2 hours at room temperature. Serum samples were diluted 1:500 in PBS and added in duplicate at 100 μL per well. The plates were incubated at room temperature for 1 hour. The plates were washed as previously described. Biotin rabbit anti-rat (Dako) was diluted in PBS to 1:1000 and added at 100 μL per well. The plates were incubated at room temperature for 1 hour. The plates were washed as previously described. Peroxidase-labeled streptavidin (KPL) was diluted in PBS at 1:1000 and added at 100 μL per well for 1 hour at room temperature. The plates were washed as previously described. TMB substrate (KPL) was prepared immediately before use. 100 μL of TMB was added to each well. The plates were incubated at room temperature for approximately 10 minutes while color developed. 1N HCl was added to each well at 100 μL to stop the reaction. The plates were read at 450nm.

Infectious Virus Recovery

Samples were collected as above and frozen at ≤ 65°C until analysis. Tissues were weighed and homogenized in three volumes (w/v) of Opti-MEM® (Gibco) utilizing mechanical crushing and a single freeze thaw cycle. The supernatant was clarified by centrifugation and

ten-fold serial dilutions of samples were prepared in Opti-MEM®. Aliquots (50 μL) of each dilution were placed in 96 well plates containing BHK-21 cells (ATCC) and $TCID_{50}$ titrations were performed as described previously [28]. $TCID_{50}$ calculations were normalized per gram of tissue. The determined limit of detection (LOD) for the assay was 1.9×10^2 $TCID_{50}$/gram of tissue. The determined limit of quantification (LOQ) for the assay was 1.9×10^3 $TCID_{50}$/gram of tissue. Samples that were above the LOD but below the LOQ were determined to be putative positives, and are notated as ≤ the calculated value.

RNA Isolation from Tissues and qRT-PCR for VSV-N

Sample tissues and blood were RNALater-preserved (Applied Biosystems) and were processed for RNA isolation and qRT-PCR for VSV-nucleoprotein RNA. All tissues were homogenized for 2 minutes (20–30 Hz twice) using a single five millimeter stainless steel bead (Qiagen) in the TissueLyser II instrument (Qiagen) equipped with 2×24 adapter set (Qiagen) and spun through QIAShredders (Qiagen) according to the manufacturer's instructions. Tumor, liver, lung, spleen, ovaries, testes, brain and spinal cord were processed according to the manufacturer's instructions using the RNeasy Plus Mini Kit or RNeasy Lipid Tissue Mini Kit (Qiagen). The optional RNase-free DNase Set (Qiagen) was used according to the manufacturer's instructions with the remaining RNA isolation kits. qRT-PCR for VSV-N analysis was performed as previously described [21]. All samples and standards were run in triplicate. Samples were quantitated by comparison with a standard curve generated by amplification of 432-bp *in vitro*-transcribed RNA (MAXIscript SP6 kit; Applied Biosystems) encoding a 298-base portion of the VSV nucleocapsid gene (bases 972–1269) cloned in pCR®II-TOPO® (Invitrogen).

In vivo efficacy studies

FAT-7 tumors were established as above. When tumors reached ~0.5 cm in diameter, rats were randomized into controls (PBS) or treatment groups (n=10 per group). Depending on the in vivo experiment, different doses of viral agent (diluted in 100 μL PBS) or vehicle were administered either IT or intravenously (IV). For all in vivo experiments, rats were euthanized when any one of the following criteria were met: a) neurotoxicity, b) tumor volume exceeded 10% of body weight, c) ulcerated tumors, or d) if animal was unable to reach food or water, 15% body weight loss, or the tumor volume exceeded 10% of body weight. Both tumor progression and time to sacrifice were analyzed.

Statistical analyses

Data are presented as means +/− SD (for in vitro studies) or SEM (in vivo studies). In vitro experiments were performed in triplicate and repeated twice, unless otherwise specified. Differences in means among groups were compared by analysis of variance, and pair wise comparisons were performed using the Student's T test or Tukey–Kramer method. Survival curves were generated using the Kaplan-Meier method and compared using the log-rank test. Differences were considered statistically significant at $p< 0.05$.

RESULTS

In vitro cytotoxicity, viral replication and gene expression of recombinant VSV-r-IFN-β and VSV-m-IFN-β on rat and mouse squamous cell carcinoma cell lines

Rat (FAT-7) and mouse (SCC-VII) SCC cells were exposed to VSV-r/m-IFN-β at different MOIs and viability/cytotoxicity was assessed at 24, 48, and 72 hrs time points. VSV-r/m-IFN-β significantly inhibited viability and induced cytotoxicity in a dose and time dependent manner in FAT-7 (Fig 1 A, B) and SCC-VII cells (Fig 2 A, B). VSV-r-IFN-β (MOI=1) inhibited FAT-7 viability by 80% ($p< 0.0001$) and induced cytotoxicity (70% vs. 6% in controls, $p< 0.0001$) at an MOI of 1, at 48 hours (Fig. 1 A, B). Similar results were observed in SCC-VII cells, where VSV-m-IFN-β (MOI=1) resulted in a 79.5% reduction in viability at 48 hours and significant cytotoxic effects (56.7% vs. 5.2%), compared to controls ($p<0.0001$ for both, Fig. 2 A, B). Statistically significant increased cytotoxicity was observed at MOIs of 0.01 and higher, both in FAT-7 ($p=0.0019$) and in SCC VII cells ($p=0.013$). The cytotoxic effects were observed as early as 24 hours after infection, and were prominent at 48 hours and later in the rat and mouse SCC cell lines (Figs 1.C, 2.C). Hypoxia did not significantly affect viral induced cytotoxicity in FAT-7 and SCC-VII cells (Figs 1.D & 2.D, respectively), and did not affect in vitro viral replication (data not shown).

Next, replication of VSV-r/m-IFN-β in rodent cell lines was assessed at different time points after infection[29]. As shown in Figure 1.E & 2.E, rat and mouse viruses efficiently replicated in FAT-7 and SCC-VII cells, respectively, as evaluated by determination of viral titers 24 and 48 hours after viral infection. Viral titers at 48 hours post-infection were 5.43×10^9 in FAT-7 cells (Fig. 1. E) vs. 3.71×10^9 in SCC-VII cells (Fig. 2. E). Viral induced transgene expression was confirmed by determination of IFN-β protein in the conditioned media of FAT-7 and SCC VII cells by western blot, 24 hours after viral infection (MOI 5 & 10; Figs. 1. F & 2. F).

The above results suggest that both mouse and rat SCCC cells are susceptible to VSV-IFN-β cytopathic effects, and both are permissive to viral replication. We observed, however, that FAT-7 cells were associated with more efficient viral replication and cytotoxic effects than SCC-VII cells (Fig. 1 B, E vs. Fig. 2. B, E). We then assessed differences in viability, cytotoxicity and viral replication between recombinant VSV vectors expressing human and rat IFN-β in FAT-7 cell lines. As seen in Fig. 3.A and B, the cytotoxic effects of VSV-r-IFN-β and VSV-h-IFN-β were comparable (p= NS). Similarly, FAT-7 cells were permissive to viral replication of both the human and rat variants of the virus, but titers of VSV-h-IFN-β were higher than VSV-r-IFN-β (Fig. 3. C).

In vivo safety and virus biodistribution after local administration of VSV-r-IFN-β or VSV-h-IFN-β in tumor and non-tumor bearing rats

Fat-7 tumors were established in immunocompetent Fisher-344 rats, as in materials and methods. Tumors became palpable at approximately day 21 after tumor cell administration. To determine the maximum tolerated dose (MTD) and no observable adverse effects level (NOAEL), rats (n=6 per group) were either administered saline (control group), 1×10^8 $TCID_{50}$, 1 × 109 $TCID_{50}$, 1 × 1010 $TCID_{50}$ VSV-r-IFN-β intratumorally (IT), or

subcutaneously (s.c, non-tumor bearing rats). During the study, no animal deaths were observed due to toxicity; one animal was euthanized due to tumor ulceration not related to viral infection. No episodes of neurotoxicity were observed after local administration of the highest virus dose level tested (1×10^{10} $TCID_{50}$) in tumor or non-tumor bearing rats. We observed that following s.c injection of 10^{10} VSV-r-IFN-β in non-tumor bearing rats, a small focal subcutaneous cellulitis was observed which resolved spontaneously. No significant weight changes were observed in treated animals.

To determine the presence of infectious virus in tumor or non-tumor tissues after VSV-r-IFN-β, administration, a group of rats (n=8) was given intratumoral VSV-r-IFN-β, and brain, spleen and tumor samples were collected 48 hours after treatment. No virus was detected in brain or spleen samples, while infectious virus was detected in 5 of 8 tumor samples in rats treated with VSV-***r***-IFN-β (Fig. 4. A). Infectious viral particles were undetectable (below limit of detection), at day 28/29 of treatment (not shown). Tissue biodistribution was further characterized by determination of VSV N(nucleoprotein) RNA by qRT-PCR in rats treated with the highest dose of oncolytic virus.(10^{10} $TCID_{50}$). As shown in Figure 4. B, VSV-N was detected at day 2 in tumor (8 of 8), spleen (4 of 8), ovary (3 of 4), spinal cord (3 of 8), and blood (6 of 11) samples, while in other organs the virus was not detected. At day 28/29 after treatment, virus was not detected (only tissues that were positive on day 2 were tested), except for one tumor sample.

Similar results were observed in tumor bearing rats treated with VSV-h-IFN-β (Fig. 5). Rats (n=6 per group) were treated with 1×10^{8} or 1×10^{9} $TCID_{50}$VSV-h-IFN-β and followed out either two days or one month for the highest dose. No signs of general toxicity or neurotoxicity were observed throughout the study, and no treatment-related deaths were observed. Infectious virus was detected in 5 of 6 tumor samples, and in none of the brain or spleen tissues at day2 in rats treated with 1×10^{9} $TCID_{50}$ VSV-h-IFN-β (Fig. 5. A). Viral RNA was detected at day 2 in tumor (6 of 6), spleen (5 of 6), ovary (3 of 3), spinal cord (1 of 6), and blood (4 of 9). Virus in the spleen was detected at or below the limits of quantification (Fig. 5. B).

Additional studies were performed in non-tumor bearing rats, which were treated with a single subcutaneous (below the jaw line) injection of escalating doses (1×10^{7}, 1×10^{8}, 1×10^{9} $TCID_{50}$) of VSV-h-IFN-β, or one dose (1×10^{9} $TCID_{50}$) of VSV-h-IFN-β or VSV-r-IFN-β (n=3 per group). No signs of acute general toxicity, neurotoxicity, or significant weight changes were observed in the treated animals. qRT-PCR for VSV-N RNA from blood, liver, spleen, ovary, testicle, brain, and spinal cord were below the limit of detection of the assay (not shown).

Blood was obtained for hematological and biochemical studies, to assess whether VSV treatment is associated with hematological, renal or hepatic toxicity. No clinically significant differences between -tumor or non-tumor bearing- treated and control rats were detected (data not shown).

Antibody Production

Blood from (tumor bearing and tumor free) rats, treated with the rat or human IFN expressing VSV vectors was obtained at days 2 and 28/29 of treatment, for determination of serum anti VSV antibody by ELISA. Anti VSV antibody was not detected from day 2 serum (not shown), while a dose dependent increase in antibody titers was observed at day 28/29, in tumor bearing rats treated with the rat (Fig. 4. C) or human (Fig. 5. C) VSV-IFN-β. Likewise, a robust (anti-VSV) antibody response was observed in non-tumor bearing rats at day 28/29 after treatment in all dose levels (data not shown).

In vivo antitumor effects of VSV-r-IFN-β and VSV-h-IFN-β

The FAT-7 was established as in materials and methods. After tumors reached approximately 0.5 cm, single intratumoral (IT) injections of VSV-r-IFN-β at three different doses (5×10^7, 5×10^8, 5×10^9 PFUs) were administered, and changes in tumor volume were assessed. Rats treated with a dose of 5×10^8 PFUs had a significant delay in tumor growth ($p<0.0001$ at day 43; Fig. 6. A), as well as time to sacrifice ($p=0.0008$; Fig. 6. B), compared to controls. Interestingly, rats treated at a higher dose (5×10^9 PFU) did not have additional benefit in tumor reduction or time to sacrifice. Next, we determined the effects of single vs. two intratumoral injections of VSV-r-IFN-β (at a dose of 5×10^8 PFU) as well as the effects of intravenous administration of the virus (one dose of 5×10^8 PFU) in tumor bearing rats. Treatment with 1 or 2 IT doses or 1 IV dose of VSV-r-IFN-β was associated with significant delay in tumor growth ($p< 0.0001$ at day 43; Fig. 6. C), and improvement in time to sacrifice ($p <0.05$, Fig. 6. D), compared to controls.

Finally, we investigated the effects of VSV-h(uman)-IFN-β in the syngeneic model. Tumor bearing rats were treated with either IT or IV VSV-h-IFN-β (one dose of 5×10^8 PFUs) around day 21 after tumor implantation. As shown in figure 7.A & B, both IT and IV administration of VSV-h-IFN-β were associated with significant tumor delaying effects ($p=0.0002$ VSV-IT vs. ctrl; $p=0.0004$, VSV-IV vs. ctrl at day 38), as well as improved survival (time to sacrifice) compared to mock treated animals ($p<0.0001$). No significant toxicity was observed in VSV-h-IFN-β treated animals.

DISCUSSION

Significant progress has been made in the field of oncolytic virotherapy, with an increasing number of oncolytic viral vectors showing promising antitumor activity and entering phase III clinical studies. Squamous cell carcinoma of the head and neck is an ideal model for the development of oncolytic virotherapy strategies because:

- Recurrent disease at the primary site or in the neck is common following initial therapy,
- The recurrent disease is most often accessible for local injection of the vector, and
- Outcomes are poor with the limited therapeutic options available for these patients

VSV is a potent oncolytic agent that has shown antitumor effects in several tumor types in vitro and in vivo, including SCC of the head and neck [13, 15, 18, 23, 30–34]. VSV-IFN-β is a

second generation recombinant oncolytic VSV that has an improved safety window, as previously reported [18]. In this report, we provided preclinical evidence of the safety and activity of VSV-IFN-β in an immunocompetent, syngeneic rat model of head and neck squamous cell carcinoma.

In vitro cytotoxicity and viral replication were demonstrated in murine and rat SCC cell lines, and transgene expression of IFN-β was confirmed in the above cell lines after infection with species specific VSV-IFN-β. The cytotoxic effects of VSV-IFN-β were not significantly affected by hypoxia, which provides a potential therapeutic advantage, as hypoxia is a common feature of advanced head and neck tumors, and is associated with poor prognosis [35–37].

Administration of both intratumoral or intravenous VSV-h-IFN-β or VSV-r-IFN-β was found to be safe. No significant toxicity or treatment related deaths were observed in the rats treated with either rat or human VSV-IFN-β. Because we are proposing a phase I clinical trial to investigate safety of intratumoral (IT) administration of VSV-h-IFN-β virus in patients with advanced, refractory HNC, our preclinical studies focused mainly on IT administration of virus in rats bearing SCC tumors in the neck area. No significant toxicity was seen in rats treated at doses up to 10^{10} $TCID_{50}$ of VSV-r-IFN-β and up to 109 $TCID_{50}$ of VSV-h-IFN-β. Based on the above results, the No Observable Adverse Event Level (NOAEL) was determined to be greater than or equal to 10^{10} $TCID_{50}$ VSV-r-IFN-β when delivered IT, in Fischer-344 rats, either tumor free or those bearing the SCCHN tumor FAT-7 s.c. For in vivo experiments using VSV-h-IFN-β, the NOAEL in tumor and non-tumor bearing rats was determined to be greater or equal to 1×10^{9} $TCID_{50}$. The data presented in the current study further support the preclinical safety profile of this virus previously reported in other models [18, 21].

Biodistribution studies demonstrated higher levels of VSV-IFN-β (human or rat) RNA (by qRT-PCR) in tumors, compared to non-tumor bearing tissues, such as spleen, ovary and bloodViable viral particles, however, were recovered only in tumor bearing organs, suggesting that while VSV-IFN-β may transiently infect both tumor and non-tumor tissues, viral replication and cytotoxic effects occur predominantly in tumors, due to the protective -antiviral- effects of virus induced IFN-β expression in normal tissues. No clinically significant hematological or biochemical side effects were observed in treated rats, which correlate well with lack of systemic toxicity or treatment related deaths in our studies. As expected, antibody formation was detected at day 28/29, in a dose dependent manner.

In vivo, both VSV-r-IFN-β and VSV-h-IFN-β were associated with significant delays in progression in rats bearing aggressive FAT-7 tumors. We saw no significant differences in the antitumor effects between intratumoral vs. intravenous administration of one dose of virus, or significant differences in antitumor effects between one vs. two intratumoral administrations of VSV-r-IFN-β. We did not observe tumor eradication after intratumoral or intravenous treatment. This may be due to development of host antiviral immunity, which prevented prolonged viral replication. However, the observed effects were associated with improvement in survival in the treated rats.

In conclusion, intratumoral administration of VSV-r-IFN-β or VSV-h-IFN-β in immunocompetent rats bearing syngeneic squamous cell tumors was feasible and safe at the doses tested. The safety and efficacy of VSV-IFN-β in this syngeneic model showed in this report provides a preclinical rationale for the clinical evaluation of this viral vector in human squamous cell carcinoma of the head and neck. Further characterization of VSV-IFN-β biodistribution after systemic administration and repeated administration in vivo are underway, as well as a first in man phase I trial of VSV-h-IFN-β in human squamous cell carcinoma of the head and neck.

Acknowledgments

Funding: Sylvester Comprehensive Cancer Center, *Bankhead-Coley Cancer Research Program, Florida Department of Health (***09BR01)**. NCI/NIH Mayo Clinic Comprehensive Cancer Center grant (P30CA015083).

References

1. Porosnicu M, Mian A, Barber GN. The oncolytic effect of recombinant vesicular stomatitis virus is enhanced by expression of the fusion cytosine deaminase/uracil phosphoribosyltransferase suicide gene. Cancer research. 2003; 63(23):8366–76. [PubMed: 14678998]
2. Haddad RI, Shin DM. Recent advances in head and neck cancer. N Engl J Med. 2008; 359(11): 1143–54. [PubMed: 18784104]
3. Shin DM, Khuri FR. Advances in the management of recurrent or metastatic squamous cell carcinoma of the head and neck. Head Neck. 2011
4. O'Rorke MA, Ellison MV, Murray LJ, Moran M, James J, Anderson LA. Human papillomavirus related head and neck cancer survival: A systematic review and meta-analysis. Oral Oncol. 2012
5. de Andrade DA, Machiels JP. Treatment options for patients with recurrent or metastatic squamous cell carcinoma of the head and neck, who progress after platinum-based chemotherapy. Curr Opin Oncol. 2012; 24(3):211–7. [PubMed: 22498572]
6. Bourhis J, Le Maitre A, Baujat B, Audry H, Pignon JP. Individual patients' data meta-analyses in head and neck cancer. Curr Opin Oncol. 2007; 19(3):188–94. [PubMed: 17414635]
7. Brockstein B, Haraf DJ, Rademaker AW, et al. Patterns of failure, prognostic factors and survival in locoregionally advanced head and neck cancer treated with concomitant chemoradiotherapy: a 9-year, 337-patient, multi-institutional experience. Ann Oncol. 2004; 15(8):1179–86. [PubMed: 15277256]
8. Posner MR, Hershock DM, Blajman CR, et al. Cisplatin and fluorouracil alone or with docetaxel in head and neck cancer. N Engl J Med. 2007; 357(17):1705–15. [PubMed: 17960013]
9. Salama JK, Seiwert TY, Vokes EE. Chemoradiotherapy for locally advanced head and neck cancer. J Clin Oncol. 2007; 25(26):4118–26. [PubMed: 17827462]
10. Liu TC, Galanis E, Kirn D. Clinical trial results with oncolytic virotherapy: a century of promise, a decade of progress. Nat Clin Pract Oncol. 2007; 4(2):101–17. [PubMed: 17259931]
11. Eager RM, Nemunaitis J. Clinical development directions in oncolytic viral therapy. Cancer gene therapy. 2011; 18(5):305–17. [PubMed: 21436867]
12. Barber GN. VSV-tumor selective replication and protein translation. Oncogene. 2005; 24(52): 7710–9. [PubMed: 16299531]
13. Shin EJ, Chang JI, Choi B, et al. Fusogenic vesicular stomatitis virus for the treatment of head and neck squamous carcinomas. Otolaryngol Head Neck Surg. 2007; 136(5):811–7. [PubMed: 17478221]
14. Shin EJ, Wanna GB, Choi B, et al. Interleukin-12 expression enhances vesicular stomatitis virus oncolytic therapy in murine squamous cell carcinoma. Laryngoscope. 2007; 117(2):210–4. [PubMed: 17204993]

15. Sung CK, Choi B, Wanna G, Genden EM, Woo SL, Shin EJ. Combined VSV oncolytic virus and chemotherapy for squamous cell carcinoma. The Laryngoscope. 2008; 118(2):237–42. [PubMed: 18043494]
16. Clarke DK, Cooper D, Egan MA, Hendry RM, Parks CL, Udem SA. Recombinant vesicular stomatitis virus as an HIV-1 vaccine vector. Springer Semin Immunopathol. 2006; 28(3):239–53. [PubMed: 16977404]
17. Johnson JE, Nasar F, Coleman JW, et al. Neurovirulence properties of recombinant vesicular stomatitis virus vectors in non-human primates. Virology. 2007; 360(1):36–49. [PubMed: 17098273]
18. Obuchi M, Fernandez M, Barber GN. Development of recombinant vesicular stomatitis viruses that exploit defects in host defense to augment specific oncolytic activity. J Virol. 2003; 77(16): 8843–56. [PubMed: 12885903]
19. Li H, Peng KW, Dingli D, Kratzke RA, Russell SJ. Oncolytic measles viruses encoding interferon beta and the thyroidal sodium iodide symporter gene for mesothelioma virotherapy. Cancer gene therapy. 2010; 17(8):550–8. [PubMed: 20379224]
20. Murata M, Nabeshima S, Kikuchi K, Yamaji K, Furusyo N, Hayashi J. A comparison of the antitumor effects of interferon-alpha and beta on human hepatocellular carcinoma cell lines. Cytokine. 2006; 33(3):121–8. [PubMed: 16522372]
21. Jenks N, Myers R, Greiner SM, et al. Safety studies on intrahepatic or intratumoral injection of oncolytic vesicular stomatitis virus expressing interferon-beta in rodents and nonhuman primates. Hum Gene Ther. 2010; 21(4):451–62. [PubMed: 19911974]
22. Majid AM, Ezelle H, Shah S, Barber GN. Evaluating replication-defective vesicular stomatitis virus as a vaccine vehicle. Journal of virology. 2006; 80(14):6993–7008. [PubMed: 16809305]
23. Fernandez M, Porosnicu M, Markovic D, Barber GN. Genetically engineered vesicular stomatitis virus in gene therapy: application for treatment of malignant disease. J Virol. 2002; 76(2):895–904. [PubMed: 11752178]
24. Elsby R, Heiber JF, Reid P, Kimball SR, Pavitt GD, Barber GN. The alpha subunit of eukaryotic initiation factor 2B (eIF2B) is required for eIF2-mediated translational suppression of vesicular stomatitis virus. Journal of virology. 2011; 85(19):9716–25. [PubMed: 21795329]
25. Balachandran S, Barber GN. Defective translational control facilitates vesicular stomatitis virus oncolysis. Cancer Cell. 2004; 5(1):51–65. [PubMed: 14749126]
26. Merchan JR, Kovacs K, Railsback JW, et al. Antiangiogenic activity of 2-deoxy-D-glucose. PLoS One. 2010; 5(10):e13699. [PubMed: 21060881]
27. Heiber JF, Barber GN. Vesicular stomatitis virus expressing tumor suppressor p53 is a highly attenuated, potent oncolytic agent. Journal of virology. 2011; 85(20):10440–50. [PubMed: 21813611]
28. Hadac EM, Peng KW, Nakamura T, Russell SJ. Reengineering paramyxovirus tropism. Virology. 2004; 329(2):217–25. [PubMed: 15518802]
29. Ebert O, Shinozaki K, Kournioti C, Park MS, Garcia-Sastre A, Woo SL. Syncytia induction enhances the oncolytic potential of vesicular stomatitis virus in virotherapy for cancer. Cancer Res. 2004; 64(9):3265–70. [PubMed: 15126368]
30. Shin EJ, Wanna GB, Choi B, et al. Interleukin-12 expression enhances vesicular stomatitis virus oncolytic therapy in murine squamous cell carcinoma. The Laryngoscope. 2007; 117(2):210–4. [PubMed: 17204993]
31. Wu Y, Lun X, Zhou H, et al. Oncolytic efficacy of recombinant vesicular stomatitis virus and myxoma virus in experimental models of rhabdoid tumors. Clin Cancer Res. 2008; 14(4):1218–27. [PubMed: 18281557]
32. Goel A, Carlson SK, Classic KL, et al. Radioiodide imaging and radiovirotherapy of multiple myeloma using VSV(Delta51)-NIS, an attenuated vesicular stomatitis virus encoding the sodium iodide symporter gene. Blood. 2007; 110(7):2342–50. [PubMed: 17515401]
33. Wu L, Huang TG, Meseck M, et al. rVSV(M Delta 51)-M3 is an effective and safe oncolytic virus for cancer therapy. Hum Gene Ther. 2008; 19(6):635–47. [PubMed: 18533893]

34. Ramsburg E, Publicover J, Buonocore L, et al. A vesicular stomatitis virus recombinant expressing granulocyte-macrophage colony-stimulating factor induces enhanced T-cell responses and is highly attenuated for replication in animals. J Virol. 2005; 79(24):15043–53. [PubMed: 16306575]

35. Brizel DM, Dodge RK, Clough RW, Dewhirst MW. Oxygenation of head and neck cancer: changes during radiotherapy and impact on treatment outcome. Radiother Oncol. 1999; 53(2):113–7. [PubMed: 10665787]

36. Nordsmark M, Bentzen SM, Rudat V, et al. Prognostic value of tumor oxygenation in 397 head and neck tumors after primary radiation therapy. An international multi-center study Radiother Oncol. 2005; 77(1):18–24.

37. Rajendran JG, Schwartz DL, O'Sullivan J, et al. Tumor hypoxia imaging with [F-18] fluoromisonidazole positron emission tomography in head and neck cancer. Clinical cancer research: an official journal of the American Association for Cancer Research. 2006; 12(18):5435–41. [PubMed: 17000677]

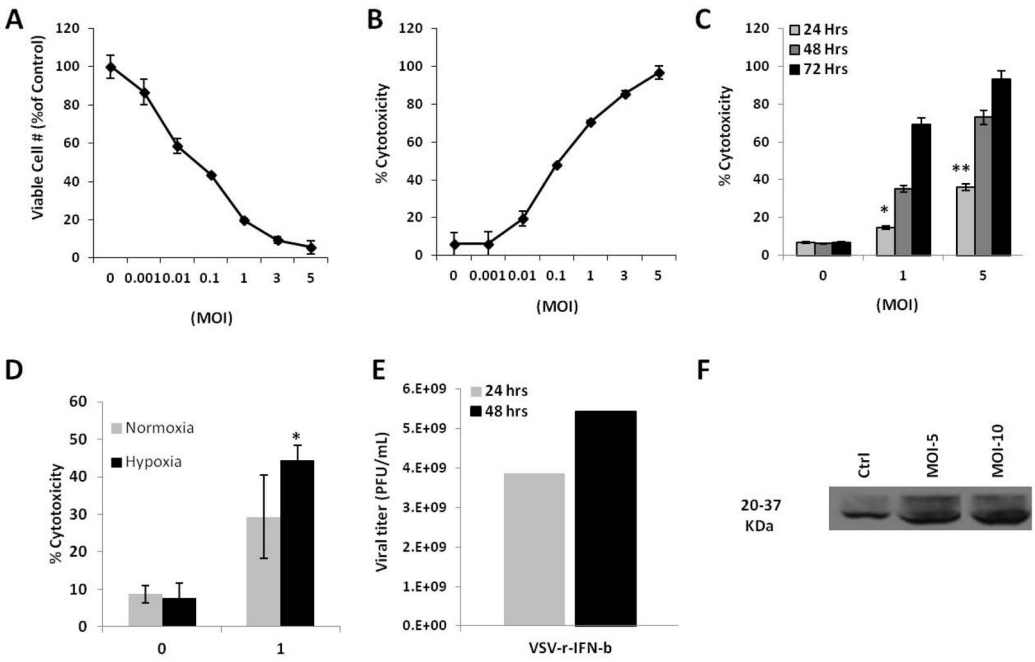

FIGURE 1. Effects of VSV-r-IFN-β on FAT-7 cells in vitro

A, B. Dose Response. Cells were infected with VSV-r-IFN-β at different MOI's and viable cell number (percent of control, **A**) and percent cytotoxicity (**B**) were determined. **C**. Time dependent cytotoxicity. Cells were infected with VSV-r-IFN-β and % cytotoxicity was determined at 24 (light grey bars), 48 (dark grey bars) and 72 hrs (black bars); ***** p= 0.14 (MOI=1 vs. control, 24 hours); ** p= 0.0008 (MOI=5 vs. control, 24 hours). **D**. Effects of VSV-r-IFN-β on cytotoxicity, during normoxia and hypoxia, at 48 hrs. * p= 0.09 (MOI=1 hypoxia vs. normoxia). Experiments in A-D were performed in triplicate, and repeated at least twice. **E**. *In vitro* viral replication. VSV-r-IFN-β titers were determined at 24 and 48 hours after infection by plaque forming assay (duplicate experiments). **F**. Western blot analysis of VSV-r-IFN-β expression in the FAT-7 conditioned medium (24 hours) after viral transduction at MOI=5 and 10.

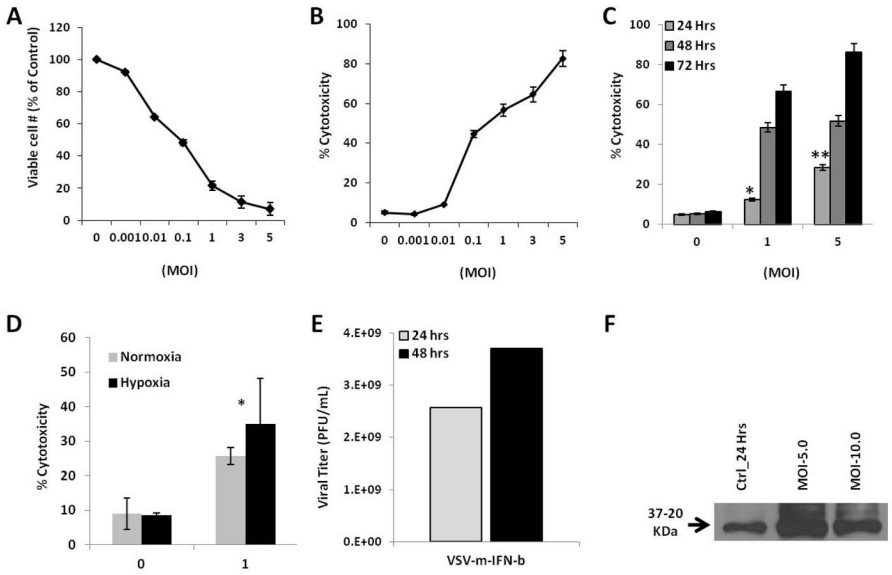

FIGURE 2. Effects of VSV-m-IFN-β on SCC VII cells in vitro

A, B. Dose Response. Cells were infected with VSV-m-IFN-β at different MOI's and viable cell number (percent of control, **A**) and percent cytotoxicity (**B**) were determined. **C**. Time dependent cytotoxicity. Cells were infected with VSV-m-IFN-β and % cytotoxicity was determined at 24 (light grey bars), 48 (dark grey bars) and 72 hrs (black bars). *****p= 0.05 (MOI=1 vs. control, 24 hours); ****** p= 0.0003 (MOI=5 vs. control, 24 hours). **D**. Effects of VSV-m-IFN-β on cytotoxicity, during normoxia and hypoxia, at 48 hrs. * p= 0.29. Experiments in A-D were performed in triplicate, and repeated at least twice. **E**. *In vitro* viral replication. VSV-m-IFN-β titers were determined at 24 and 48 hours after infection by plaque forming assay (duplicate experiments). **F**. Western blot analysis of VSV-m-IFN-β expression in the SCC VII conditioned medium (24 hours) after viral transduction at MOI=5 and 10.

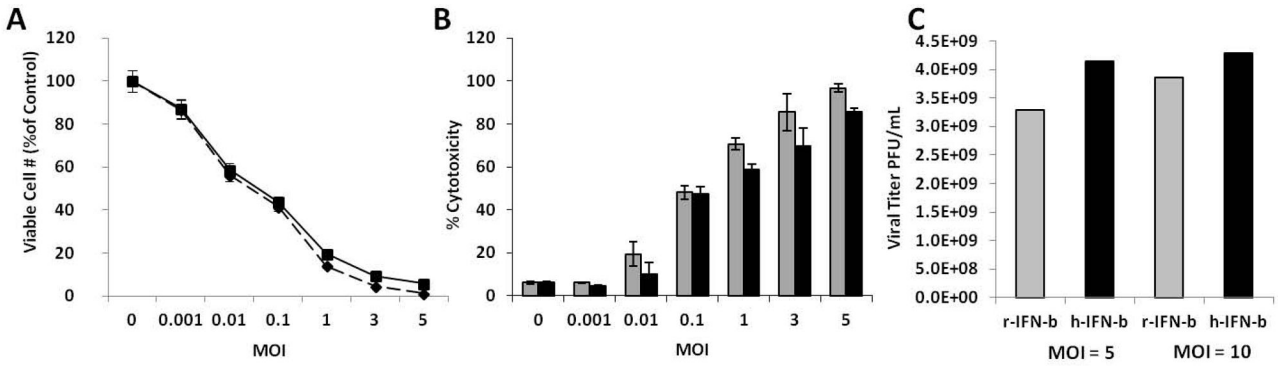

FIGURE 3. In vitro cytotoxicity and viral replication of human or rat VSV-IFN-β on FAT-7 cells

FAT-7 cells were exposed to VSV-h-IFN-β or VSV-r-IFN-β at different MOIs and viability and cytotoxicity at 48 hours were assessed. **A.** Effects of VSV-h-IFN-β (solid lane) or VSV-r-IFN-β (broken lane) on viable cell number (% of control). **B.** Effects of VSV-h-IFN-β (black bars) or VSV-r-IFN-β (grey bars) on FAT-7 cytotoxicity at 48 hours. Experiments were performed in triplicate, and repeated at least twice **C.** *In vitro* viral replication of VSV-r-IFN-β (grey bars) and VSV-h-IFN-β (black bars) in FAT-7 Cells. Viral titers were determined by plaque forming assay at 48 hrs and at MOI-5 or 10 (duplicate experiments).

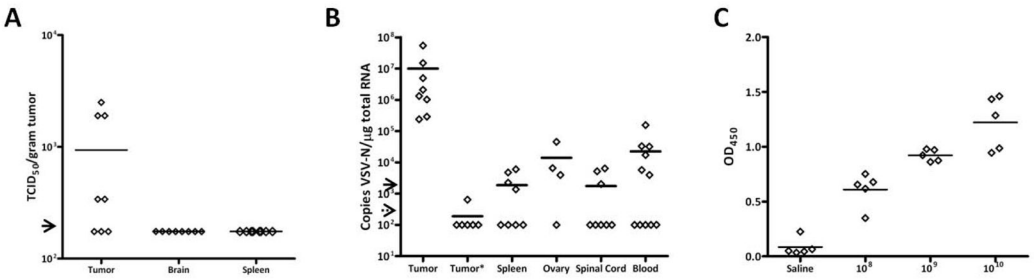

FIGURE 4. Tissue biodistribution and anti-VSV antibody production after intratumoral administration of VSV-r-IFN-β in immunocompetent rats

Fisher 344 rats bearing FAT-7 tumors in the neck area (as in materials and methods) were given one intratumoral injection of VSV-r-IFN-β (1×10^{10}TCID$_{50}$ per rat), and tumors and tissues were harvested at day 2 (n=8) and 28/29 (n=6) after treatment. **A.** Recovery of VSV-r-IFN-β from tumor, brain and spleen tissues harvested from rats at day 2. Viral titers are displayed as TCID$_{50}$ per gram of tissue; arrow represents the assay's limit of detection – LOD- (1.92×10^2 TCID$_{50}$/g tissue). **B.** Analysis of tissue biodistribution (assessed by quantitative RT-PCR of VSV-N RNA) after treatment with VSV-r-IFN-β. Total RNA was isolated from day 2 and 28/29 rats' tumors and tissues. Data are displayed as copy number VSV-N RNA per µg or RNA. Tumor *: day 28/29 tumor sample. Dark line arrow=LOD, limit of detection; dotted line arrow=LOQ, limit of quantification). **C.** Anti-VSV antibody production. Anti-VSV ELISA was performed on day 28/29 serum samples.

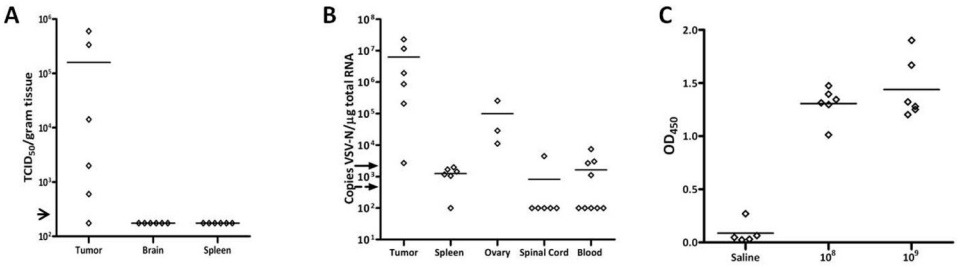

FIGURE 5. Tissue biodistribution and anti-VSV antibody production after intratumoral administration of VSV-h-IFN-β in immunocompetent rats

Fisher 344 rats bearing FAT-7 tumors in the neck area (as in materials and methods) were given one intratumoral injection of VSV-h-IFN-β (1×10^9TCID$_{50}$ per rat), and tumors tissues were harvested at day 2 (n=6) and day 28/29 (for antibody detection; n=6). **A.** Recovery of VSV-h-IFN-β from tumor, brain and spleen tissues harvested from rats at day 2. Viral titers are displayed as TCID$_{50}$ per gram of tissue; limit of detection –LOD- (arrow) = 1.92×10^2 TCID$_{50}$/g tissue. **B.** Analysis of tissue biodistribution (assessed by quantitative RT-PCR of VSV-N RNA) after treatment with VSV-h-IFN-β. Total RNA was isolated from day 2 rats' tumors and tissues. Data are displayed as copy number VSV-N RNA per 0.2 μg or RNA. Dark line arrow=LOD, limit of detection; dotted line arrow=LOQ, limit of quantification). **C.** Anti-VSV antibody production. Anti-VSV ELISA was performed on day 28/29 serum samples.

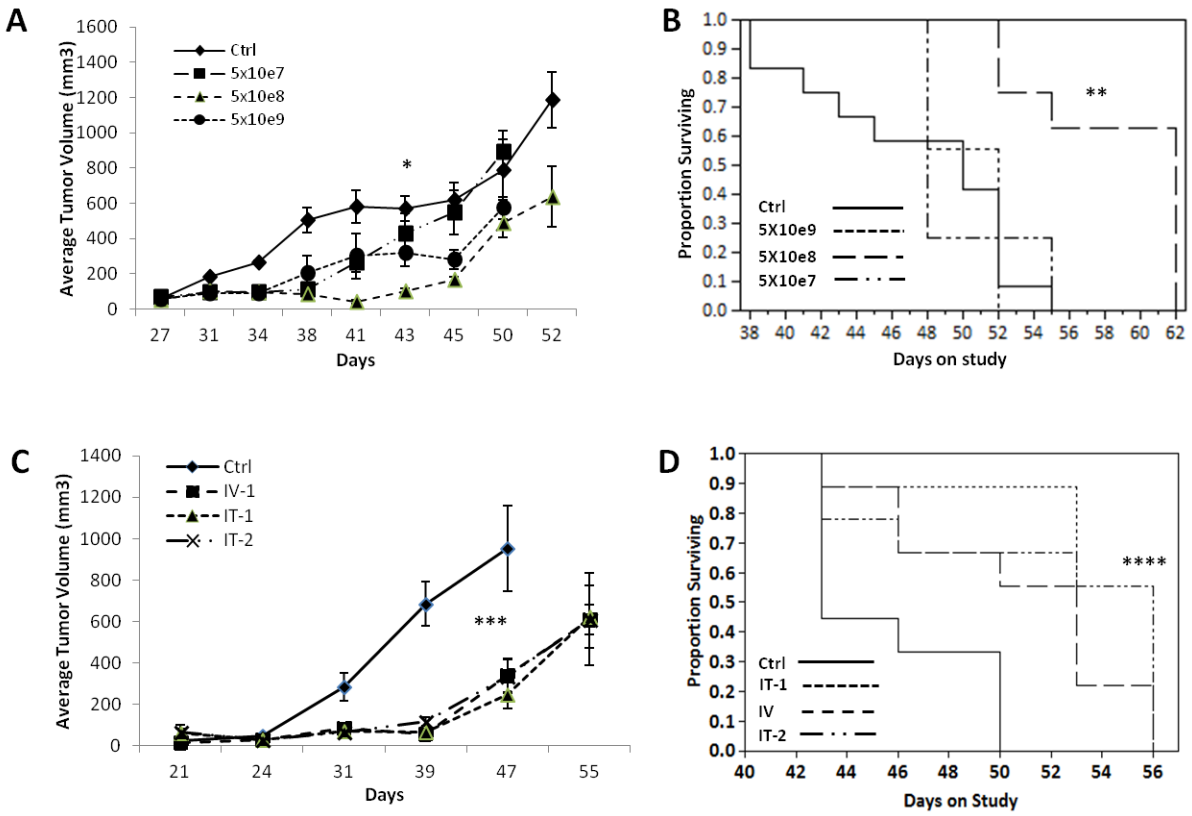

FIGURE 6. In vivo effects of VSV-r-IFN-β or VSV-h-IFN-β on tumor growth and survival in immunocompetent rats bearing FAT-7 tumors

A. Average tumor volume (mm^3) was determined in Fischer-344 (total n=40; 10 per group). Rats treated with escalating doses (5×10^7; 5×10^8 and 5×10^9 PFUs of VSV-r-IFN-β or PBS. Treatment was initiated when tumors reached approximately 5 mm in diameter. *p<0.0001 (5×10^8 vs. control). **B.** Effects of escalating doses of VSV-r-IFN-β on survival (measured by time to sacrifice, Kaplan-Meier Graph). **p=0.0008, 5×10^8 vs. control. In separate experiments, tumor bearing rats (n=40) were treated with either intratumoral (1 vs. 2 treatments, n=10 per group) or intravenous (one treatment, n=10 per group) VSV-r-IFN-β, or PBS. Treatment was initiated when tumors reached approximately 5 mm in diameter. **D.** Average tumor volume (mm^3). Tumor progression was significantly delayed in the treated groups, compared to controls (***p< 0.0001) **B.** Effects of virus treatment on survival (time to sacrifice; Kaplan-Meier Graph). **** p= 0.0003 (IT-1 vs. ctrl); p= 0.012 (IT-2 vs. ctrl); p=0.0084 (IV vs. ctrl).

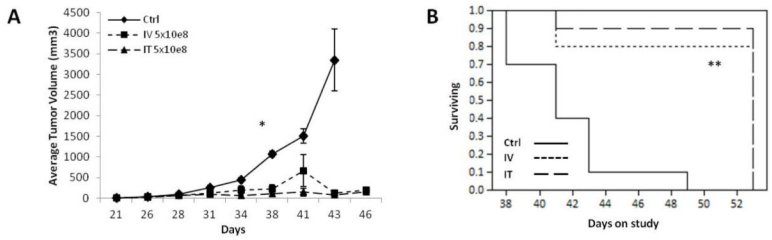

FIGURE 7. In vivo effects of VSV-h-IFN-β in syngeneic rat squamous cell carcinoma

A. Average tumor volume (mm^3) determined in Fischer-344 Rats (total n=30, 10 per group) treated with either intratumoral or intravenous VSV-h-IFN-β (5×10^8 PFUs, for one dose) or PBS. Treatment was initiated when tumors reached approximately 5 mm in diameter. *p=0.0002 VSV-IT vs. ctrl; p=0.0004, VSV-IV vs. ctrl. **B.** Effects of intratumoral or intravenous VSV-h-IFN-β (5×10^8 PFUs, for one dose) on survival (time to sacrifice). ** p<0.0001, IT/IV vs. control.